Efficiency of new ozone filters for NO_2 sensing and air depollution

M. Othman, C. Théron, Marc Bendahan, L. Caillat, C. Rivron, S. Bernardini, G. Le Chevallier, E. Chevallier, M.-P. Som, Khalifa Aguir, et al.

Sensors and Actuators B 265 (2018) 591–599

Contents lists available at ScienceDirect

Sensors and Actuators B: Chemical

journal homepage: www.elsevier.com/locate/snb

Efficiency of new ozone filters for NO_2 sensing and air depollution

M. Othman[a], C. Théron[b], M. Bendahan[a], L. Caillat[b], C. Rivron[b], S. Bernardini[a], G. Le Chevallier[b], E. Chevallier[c], M.-P. Som[c], K. Aguir[a,*], T.-H. Tran-Thi[b]

[a] Aix Marseille Univ, Université de Toulon, CNRS, IM2NP, Marseille, France
[b] NIMBE, CEA, CNRS, Université Paris-Saclay, CEA-Saclay, 91191, Gif sur Yvette Cedex, France
[c] ETHERA, 628 rue Charles de Gaulle, 38920 Crolles, France

ARTICLE INFO

Article history:
Received 26 July 2017
Received in revised form 26 February 2018
Accepted 5 March 2018
Available online 8 March 2018

Keywords:
Selectivity
NO_2 sensors
O_3 sensors
Specific filters
Nanoporous materials
Air depollution

ABSTRACT

Specific filters can be used up-stream with metal oxide (MOX) gas sensors to trap ozone and allow the selective detection of NO_2. These filtering media are based on nanoporous matrices doped with indigo-carmine that reacts selectively with O_3. The nanoporous materials, produced via the sol-gel process using functionalized silicon alkoxides as precursors, are tailored for the trapping of O_3. Depending on the nature of the filter, it is possible to entirely trap O_3 and allow NO_2 to partially pass over a certain range of concentration. For air depollution purpose, selected filters that efficiently trap both O_3 and NO_2 were exposed to harsh conditions under high concentrations of O_3 (350–475 ppb) and humidity (RH: 72%, T = 21 °C). Their trapping efficiency and lifetime are determined and compared with those of activated carbon.

1. Introduction

Tropospheric ozone is created by chemical reactions between oxides of nitrogen and volatile organic compounds. Ozone can reach unhealthy levels on hot sunny days in urban environments as well as in rural areas. According to the air quality guidelines of the World Health Organization (WHO), the maximum recommended concentration is 50 ppb for a continuous exposure and 100 ppb for a short-term exposure [1]. For nitrogen dioxide, the maximum concentration is 100 ppb for 1 h exposure and 75 ppb per day [1]. Since both oxidizing gas O_3 and NO_2 are often present at the same time in urban environments due to car exhausts, it is difficult to measure their concentrations, in particular with low-cost sensors that lack in selectivity. To enhance the selectivity of sensitive semiconductor sensors, the idea is to couple up-stream selective filters that can trap selectively either NO_2 or O_3. Many attempts have been made in the past to produce such filters that are resumed in the following state of arts.

1.1. State of arts on NO_2 and O_3 filters

Over the last decades, nitrogen dioxide (NO_2) removal from air was mainly focused on the remediation for NO_2 emission from exhaust pipes. The selective catalytic reduction widely used in car for removing sulfur dioxide (SO_2) and NO_x (NO, NO_2) from the combustion process being only efficient at high temperature, a lot of materials were tested to improve the trapping of NO_x at low temperature. Among them, activated carbon [2,3] and related materials such as char [4], Diesel soot [5], carbon black, carbon fiber [6], carbon nanotubes [7], urea-modified mesoporous carbon [8] were the most popular. When impregnated with potassium iodide (KI) or potassium hydroxide (KOH), potassium permanganate ($KMnO_4$) or Potassium nitrate (KNO_3), the efficiency of removal of NO_2 was greatly enhanced [9]. Various mixed metal oxides supported on mesoporous organosilicas SBA-15 were shown by Bandoz's group as efficient media to remove NO_2 at ambient conditions [10]. Several research groups have investigated the NO_2 adsorption on zeolites [11,12] and in particular on Zeolite Socony Mobil (ZSM-5) with a variety counter ions [13]. Szanyi et al. had shown that a yield of NO_2 removal of 165 μmol/g could be obtained with Cu ZSM-5 zeolite. More recently, metal organic framework (MOF) were shown to be of interest; Various MOFs have been studied like Zirconium-based MOF [14], Copper-based MOF [15], and an unprecedented removal capacity upwards of 1.4 g of NO_2/g of MOF was obtained by Peterson et al. using the MOF UiO-66-NH_2 [16].

* Corresponding author.
E-mail address: khalifa.aguir@im2np.fr (K. Aguir).

https://doi.org/10.1016/j.snb.2018.03.019
0925-4005/

None of the presently cited works on NO_2 filters had reported the potential co-adsorption of O_3. Activated Carbon (AC) is however known for its ability to adsorb a wide range of volatile organic compounds and gases, including NO_2 and O_3 [17,18]. A filter based on AC (Maxsorb) to selectively destroy ozone rather than nitrogen dioxide via a precise control of the temperature, was suggested by Berry et al. [19]. Other materials combining AC with oxide materials, noble-metal-supported catalysts, and various transition-metal oxides showed an enhanced ability of O_3 decomposition [20–22]. Ferrihydrite (2LFh) with accessible mesopores was also used by Mathew et al. who found 2LFh to be the most efficient candidate for O_3 removal as compared to other materials such as γFe_2O_3, Fe/ZSM-5 or commercial manganese dioxide (MnO_2) [23]. Jiang et al. showed that lichen-like porous manganese oxides (MnO_x) deposited in situ on the surface of activated carbon can exhibit a high catalytic activity and stability for ozone decomposition at room temperature and high relative humidity (RH = 60%), despite a low Mn loading [24]. Natural zeolites were also shown by Valdès et al. to display an efficient adsorption surface and catalytic properties for O_3 decomposition [25]. Blaskov et al. had shown that a Bulgarian perlite mineral coated with Ag particles deposited by spray pyrolysis could display promising catalyst properties for ozone decomposition [26]. A recent study of Yang reports the use of carbon nanotubes (CNTs) growth on quartz fibers (QF) using chemical vapor deposition, for an active ozone removal by adsorption. The ozone conversion efficiency of the CNTs/QF remained as high as 96% while AC efficiency dropped down to 40% after 10 h for an equal mass [27].

Beside Berry's work which reported the potential control of adsorption of NO_2 and O_3 on AC by heat, there is only few reports on the selectivity of O_3 filters; Pauly et al. developed nanocarbon filter composed of a mixture of carbon nanocones and nanodisks which could remove O_3 from air without major change in NO_2 concentration [28]. The capacity of the filter can increase from 7.20 to 22.19 ppm/h if the filter was flushed during 30 min with pure air (750 mL min^{-1}) after each exposure cycle (30 min, O_3:1 ppm, 750 mL min^{-1}) [29]. Because of the uneasy use of the nanocarbon filter, these authors proposed another selective filter based on the use of indigo dye. Indigo thin film was coated on an organic semiconductor sensor by sublimation of pure indigo powder [30]. It was shown that a filter thickness of 50 nm is sufficient to trap O_3 with 99% of efficiency as compared to only 5–8% for NO_2 trapping, thus allowing to greatly increasing the selectivity of the organic semiconductor towards NO_2. However, the lifetime of such thin layer is short and increasing the thickness of the layer would slower down the diffusion of NO_2 through it [31]. Moreover, the filter lifetime was not determined under humid conditions that could favor the co-trapping of NO_2. For these authors, a layer of 50 nm thick is a good compromise between a good O_3 trapping and good sensitivity of the CuPc sensor for NO_2 in non-humid conditions.

In the present work, we propose to use filters that can trap O_3 up-stream of a Metal-Oxide (MOX) sensor. These filters are functionalized nanoporous materials doped with indigo carmine for the selective trapping of O_3. The work is divided into three parts; we first describe the strategy of producing various filters with functionalized nanoporous matrices via the sol-gel process to obtain a selectivity towards NO_2 or O_3. We then quantify the ability of trapping O_3 or NO_2 using MOX sensor under various exposure conditions to a wide range of O_3 and NO_2 concentrations at different relative humidity of the gas mixtures. In the third part of the work, we will explore the potentiality of selected filters for air depollution in particular for O_3 removal. For such purpose, we will determine with breakthrough experiments the lifetime and efficiency of various O_3 filters under very harsh conditions with very high concentrations (350–475 ppb) and relative humidity (RH = 72%, T = 21 °C) and compare their efficiency to activated carbon filter.

2. Experimental

2.1. Chemicals

Various silicon derivatives, tetramethylorthosilicate (TMOS, CAS = 681-84-5, ≥ 99%), methyl trimethylorthosilicate (MeTMOS, CAS:1185-55-3, >97%), Phenyl trimethylorthosilicate (PhTMOS, CAS:2996-92-1, >97%), phenyl triethylorthosilicate (PhTEOS, CAS:780-69-8, >98%), MeOH (>99.9%) and Indigo carmine for spectroscopy (CAS:860-22-0) were purchased from Sigma-Aldrich and used as such. Chloropropyl trimethylorthosilicate (ClTMOS, CAS: 2530-87-2, >97%) and trifluororopropyl trimethylorthosilicate (F3TMOS, CAS: 429-87-2, >98%) come from TCI and EtOH (> 99.8%) from carlo Erba. The water was deionized and purified with Elix 3 and Milli-Q of Millipore.

2.2. Syntheses of doped nanoporous matrices and characterization

Nanoporous monoliths of hybrid organic-inorganic polymers doped with indigo carmine were prepared via the Sol-Gel method using as reactants one or two silicon precursors. A one-pot synthesis procedure is used for all syntheses. The concentration of indigo carmine in the aqueous solution, 70 g L^{-1}, corresponds to its solubility in water. An example of the synthesis process is given for F2 filter production: a 100 mL of Sol was produced by mixing in a flask 34.62 mL of TMOS and 4.93 mL of PhTMOS. 41.84 mL of MeOH is added and the mixture is stirred during 1 min. 18.61 mL of the aqueous solution of indigo carmine is added and the mixture is stirred during 1 h at room temperature. The proportions of the reactants TMOS/PhTMOS/MeOH/H_2O in mole fraction is 0.9/0.1/4/4 and the indigo carmine concentration is 0.0277 mol·L^{-1}. The sol was poured into specific molds that are covered with an aluminum membrane until gelation occurs. The aluminum membrane is then replaced by a porous membrane and the gels were dried in a desiccator under a N_2 stream (300 mL min^{-1}) at room temperature. After the shrinkage process, transparent and dark blue monoliths were obtained (Fig. 1). For the other filters, the proportions of the reactants, expressed in mole ratios, are given in Table 1 along with the drying duration. The concentration of indigo carmine in the final matrices varies from 0.280 to 0.324 mol dm^{-3} depending on the Sol/monolith volume shrinkage factor, which varies from 10.4 to 10.7.

The porosity parameters, specific adsorption surface area and pore volume were determined via collecting adsorption isotherms of N_2 at liquid nitrogen temperature with Autosorb I analyzer from Quantachrome. Density Functional Theory (DFT) analytical method was applied for the analyses of the porosity parameters [32].

2.3. Sensor description and experimental set-up for the detection of O_3 and NO_2 without and with various filters

The sensor is a micro-hotplate membrane (with a micro-heater and interdigitated Pt electrodes) and WO_3 sensitive layer (Fig. 2). The micro-hotplate architecture was previously developed by the IM2NP laboratory [33].The WO_3 sensitive layer with a thickness of about 50 nm was deposited by reactive magnetron RF sputtering and annealed at 450 °C during two hours to improve its nano-crystallization and stability. The gas sensing properties were studied by measuring the microsensor resistance with a Keithley 2450 source meter in a close thermo-regulated test chamber. The NO_2 and O_3 sensor sensitivity were studied under different gas concentrations, from 200 ppb to 1000 ppb for NO_2 and from 36 ppb to

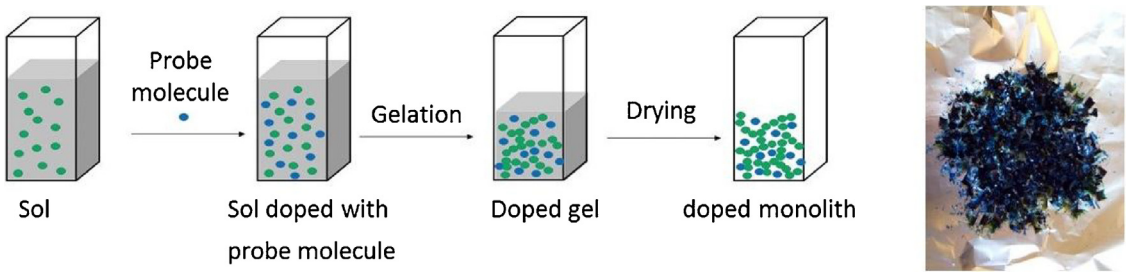

Fig. 1. Production of matrices doped with a probe-molecule, indigo carmine, via the sol-gel process. (For interpretation of the references to colour in this figure legend, the reader is referred to the web version of this article.)

Table 1
Synthesis conditions and porosity properties of the matrices doped with indigo carmine (IC). [IC] corresponds to the concentration in the Sol.

Sample	Sol composition Molar proportion	Drying time days	S_{ads} $m^2\,g^{-1}$	V_3 $cm^3\,g^{-1}$
F1	TMOS/MeOH/H_2O 1/4/4 [IC]: 0.0277 mol L^{-1}	18	880 ± 80 90% (11–20 Å) 10% (21–40 Å)	0.30 ± 0.01
F2	TMOS/PhTMOS/MeOH/H_2O 0.9/0.1/4/4 [IC]: 0.0271 mol L^{-1}	30	790 ± 60 41% (11–20 Å) 59% (21–56 Å)	0.48 ± 0.01
F3	TMOS/PhTEOS/MeOH/H_2O 0.9/0.1/4/4 [IC]: 0.0269 mol L^{-1}	37	750 ± 60 46% (11–20 Å) 54% (21–53 Å)	0.43 ± 0.01
F4	TMOS/PhTMOS/MeOH/H_2O 0.8/0.2/4/4 [IC]: 0.0267 mol L^{-1}	37	640 ± 50 36% (11–20 Å) 64% (21–56 Å)	0.40 ± 0.01
F5	TMOS/PhTEOS/MeOH/H_2O 0.85/0.15/4/4 [IC]: 0.0266 mol L^{-1}	38	560 ± 50 34% (11–20 Å) 66% (21–53 Å)	0.38 ± 0.01
F6	TMOS/ClTMOS/MeOH/H_2O 0.8/0.2/4/4 [IC]: 0.0271 mol L^{-1}	38	8 ± 2 100% (25–70 Å)	0.01
F7	TMOS/ClTMOS/MeOH/H_2O 0.5/0.5/4/4 [IC]: 0.0263 mol L^{-1}	32	Non porous	–
F8	TMOS/ClTMOS/MeOH/H_2O 0.7/0.3/4/4 [IC]: 0.0304 mol L^{-1}	15	Non porous	–
F9	TMOS/3FTMOS/MeOH/H_2O 0.7/0.3/4/4 [IC]: 0.0263 mol L^{-1}	10	460 ± 40 27% (14–20 Å) 73% (21–56 Å)	0.30 ± 0.01

210 ppb for O_3. The experimental set up allows to test the sensors under dry air, wet air and different gases, passing through the filter or not. For each concentration, the sensors were exposed to gas for 5 min and their temperature was kept constant at 275 °C. In all experiments, the gas flow was maintained at 500 sccm (Standard Cubic Centimeters per Minute). The sensor responses, *S*, were calculated using the relation (1):

$$S = \frac{R_{gas}}{R_{air}} \quad (1)$$

Where R_{air} denotes the sensor resistance under dry or humid air while R_{gas} is the sensor resistance under the gas mixture.

2.4. Measurement of filters efficiency for trapping O_3

Ozone is produced with an O_3 generator model 165 from Thermo Environmental Instruments and its concentration is measured upstream and downstream of the filter using an O_3 analyzer model 49 from Thermo Environmental Instruments. The filter is a Chromabond 3 mL syringe (9 mm of diameter, 6 cm long) filled with 1.7–1.9 g of the material to be tested. A permeable membrane is placed on each end of the syringe to filter the dust. The upstream flow rate of the cartridge is 2 mL min^{-1} and the downstream flow rate after the filter was measured for each cartridge to check that the pressure drop is about the same for all cartridges. The trapping efficiency τ, expressed in% is measured for each filter as a function of the exposure parameters; It is defined according to:

$$\tau = \frac{[O_{3up}] - [0_{3down}]}{[0_{3up}]} 100\% \quad (2)$$

Three ozone concentrations were used: 42 ± 1, 350 ± 5 ppb and 475 ± 5 ppb. The first corresponds to an average value of the ozone content in outdoor air. In order to determine a "lifetime" of few selected filters under precise conditions of use (2 L min^{-1}, HR = 50%), breakthrough curves were produced at high O_3 levels from 350 to 475 ppb. The effect of humidity of the gas mixture (RH = 50% and 72%, T = 21 ± 1 °C) was also investigated. The trapping performance was compared for various exposure times ranging from minutes to few days and up to 20 days for a few runs. A comparison was also made with a commercial RBBA activated carbon powder exposed in the same conditions to O_3.

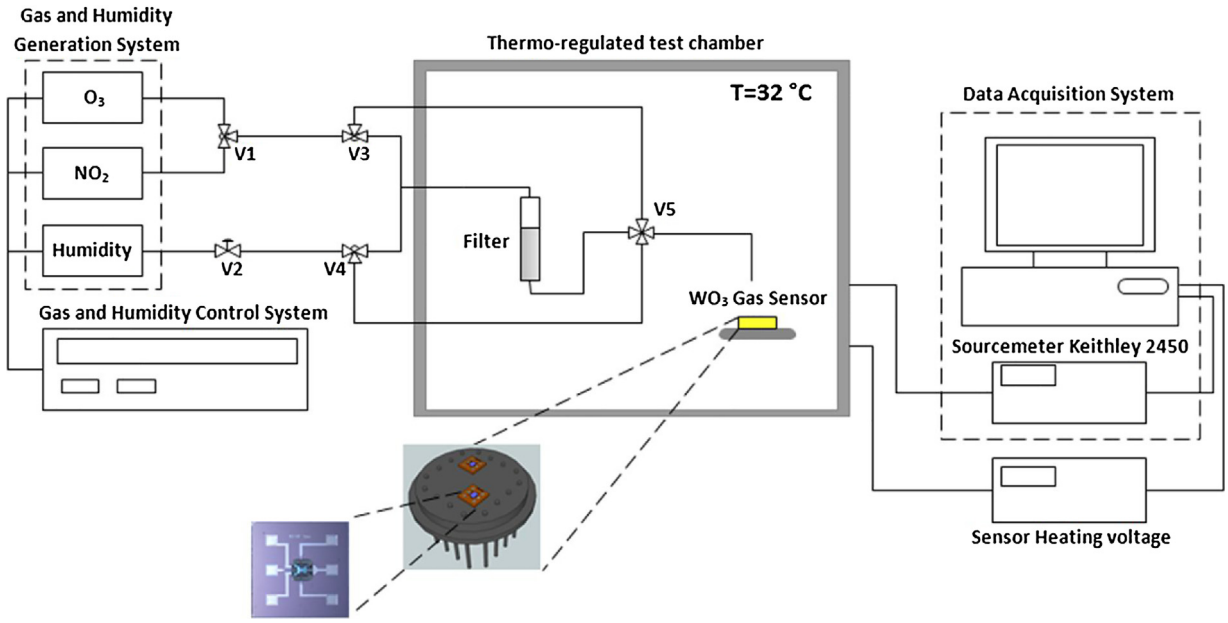

Fig. 2. Experimental setup for gas sensors and filters tests at 275 °C. The humidity inside the thermo-regulated test chamber is measured at 32 °C.

3. Results and discussion

3.1. Strategy for O_3 filters

Indigo is known to react selectively and irreversibly with ozone (O_3) by ozonolysis giving isatine groups. Alexy et al. [34] and Yasuko [35] have taken advantage of such properties to produce colorimetric sensors whose color turns from blue (indigo) to yellow (isatine), when exposed to outdoor O_3. These authors used water-soluble modified indigo immobilized in a permeable and transparent polydimethylsiloxane-polycarbonate copolymer and in a porous Vycor glass, respectively. Following the works on indigo filter and colorimetric O_3 sensors [34,35], we propose to produce an up-stream O_3 filter which could be easily used with non-selective NO_2 sensors or with any other sensors for which O_3 is an interfering gas. We here use a commercialized water-soluble indigo carmine and nanoporous matrices produced via the sol-gel process which can display high adsorption surface area comparable to certain AC. Since the ozonolysis reaction is sensitive to humidity, our strategy is to tailor the pores of the matrices in terms of size and hydrophobicity. To this end, various silicon precursors were used which contain either hydrophobic phenyl group or hydrophobic alkyl chain (chloropropyl or trifluoropropyl). The proposed filters will display a saturation warning by the gradual change of their color from dark blue (indigo carmine) to yellow (isatine).

3.2. Porosity properties of the nanoporous matrices doped with indigo carmine

The sol-gel process allows the production of a tridimensional network of pores via two reactions: hydrolysis of the silicon alkoxide precursors and condensation reaction of the resulting silanol groups, Si—OH.

$$\text{Hydrolysis}: Si(OR)_4 + 4H_2O \rightarrow Si{-}(OH)_4 + 4ROH$$

$$\text{Condensation}: 2Si(OH)_4 \rightarrow (HO)_3\text{-}Si{-}O{-}Si{-}(OH)_3 + H_2O$$

Indigo carmine was added to the solution (Sol) during a one-pot synthesis. During the condensation process, the viscosity of the Sol increases with time until gelation occurs. Before the formation of the gel, the Sol is poured into parallelepipedic molds ($16 \times 10 \times 4$ mm). After gelation and the drying process, parallelepipedic matrices ($\sim 6 \times 5 \times 2$) with dark blue color were obtained.

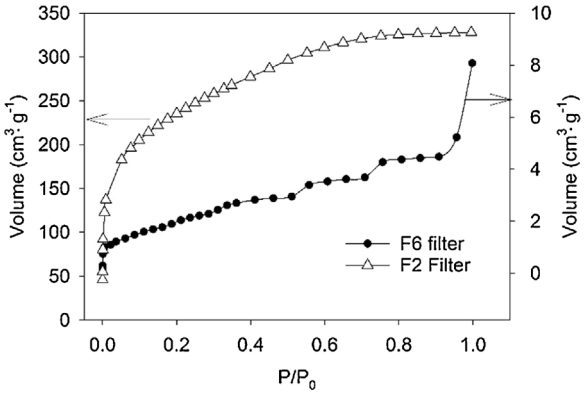

Fig. 3. Nitrogen adsorption isotherms of F2 (left scale) and F6 (right scale) filters.

When tetramethoxysilane (TMOS) is used as single precursor, the produced matrix is hydrophilic due to the uncomplete condensation reaction and the presence of residual silanol groups (Si-OH) [36]. Co-condensing TMOS with another silicon precursor bearing a phenyl group or a hydrophobic chain allows to obtain hydrophobic materials with various porosity properties depending on their proportion in the mixture. The synthesis conditions and porosity properties of the matrices doped with indigo carmine are shown in Table 1. F1 to F5 and F9 isotherms of adsorption of N_2 are typical of materials displaying both micropores (diameter <20 Å) and mesopores (20 to <500 Å, from IUPAC definition). In contrast, F6 displays the typical adsorption isotherm of nonporous materials (type II from IUPAC definition) [37] Fig. 3.

Phenyltrimethoxysilane (PhTMOS) and phenyltriethoxysilane (PhTES) only differs from their hydrolysis rate that is slower for PhTES and therefore their porosity properties are very similar. The presence of phenyl groups and long chain, due to their size, induces the formation of mesopores (20< diameter <500 Å) rather than micropores (<20 Å). Increasing the proportion of the hybrid organic-inorganic precursor thus induces an increase of the

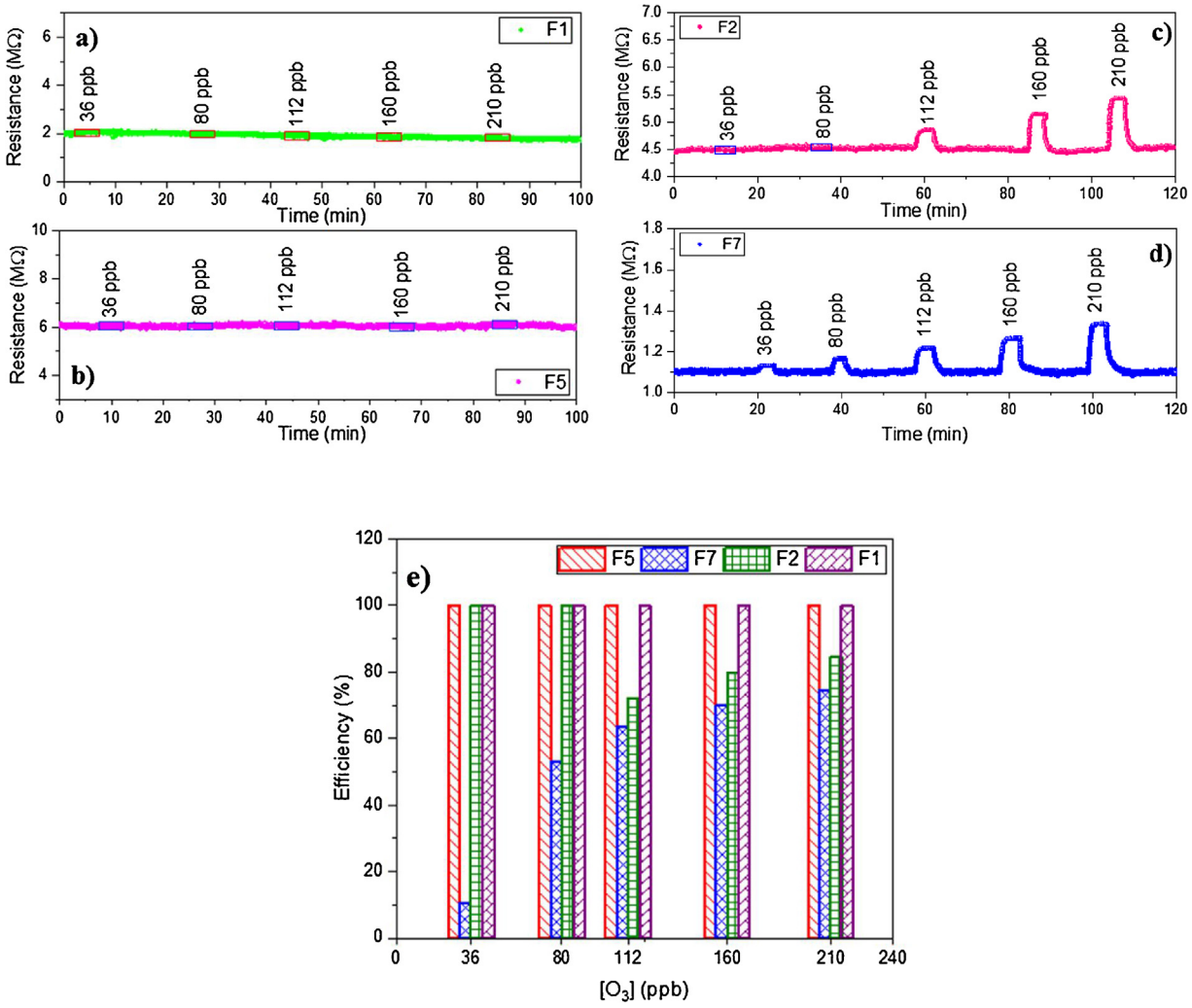

Fig. 4. Responses of the sensor at 275 °C coupled with different filters (m = 0.2 g): a) F5, b) F1, c) F2, d) F7 and e) Efficiency of the filters as a function of initial concentration. The open rectangles in Fig. 4-a--c indicates the moment the ozone is injected.

mesopores proportion and as a consequence a diminution of the adsorption surface area. For ClTMOS this effect is so important that the material become nonporous when the proportion of ClTMOS is superior to 20%. As we will see in Section 3.3, the presence of indigo carmine molecules immobilized in F6 matrix which contains 20% of ClTMOS will still allow to trap O_3 despite the very low adsorption surface area of the matrix. Due to the shrinkage with a contraction factor of ~10.4–10.7, when going from the Sol to the final matrix, the final concentration of indigo carmine varies between 0.280 and 0.324 mol dm^{-3}.

3.3. Detection of O_3 and NO_2 with various ozone filters

Semiconducting metal oxides are the most commonly sensitive materials used for gas detection. They are cheap, stable and highly sensitive and need low maintenance. Moreover, they are able to detect a large number of environmentally hazardous gases at concentrations of parts per billion (ppb), including oxidizing gases (NO_2, NO, N_2O, O_3) and reducing gases (H_2S, CO, NH_3, CH_4, SO_2). However, these metal oxides require high operating temperatures (above 300 °C) to react optimally with target gases and give fast response and recovery times. Their electrical conductance changes upon exposure to gases molecules due to the change of the carrier concentration.

Metal oxides can be n-type semiconductors as WO_3 and SnO_2 and can be *p*-type semiconductors as CuO and CoO. In n-type semiconductors where the majority of charge carriers are electrons, an increase of conductivity occurs when the sensors are exposed to a reducing gas. On the other hand, when they are exposed to an oxidizing gas, the gas reacts with the sensitive layer and thus reduce the electron charge carrier's concentration, resulting in a conductivity decrease.

We focus here on the n-type gas sensing metal-oxide material, in particular on tungsten trioxide (WO_3) which had shown particularly impressive gas sensing properties [38–42]. The n-type semiconductor WO_3 displays a native non-stoichiometric structure and the free electrons originating from oxygen vacancies contribute to the electronic conductivity change when the sensor is exposed to gases.

In order to evaluate the efficiency of O_3 trapping for an NO_2 selective detection, different measurements were carried out with each filter. For each tested filter, 1.79 g of nanoporous material (Table 2) was used upstream coupled with WO_3-based gas sensor for O_3 and NO_2 detection. The O_3 and NO_2 concentration range was varied between 36–210 ppb and from 0.2 to 1.0 ppm, respectively. In both cases, the flux mixture is 500 sccm.

Table 2 illustrates the trapping efficiency of the filters (for $[O_3]$ = 210 ppb and $[NO_2]$ = 1 ppm) as well as their effect on the

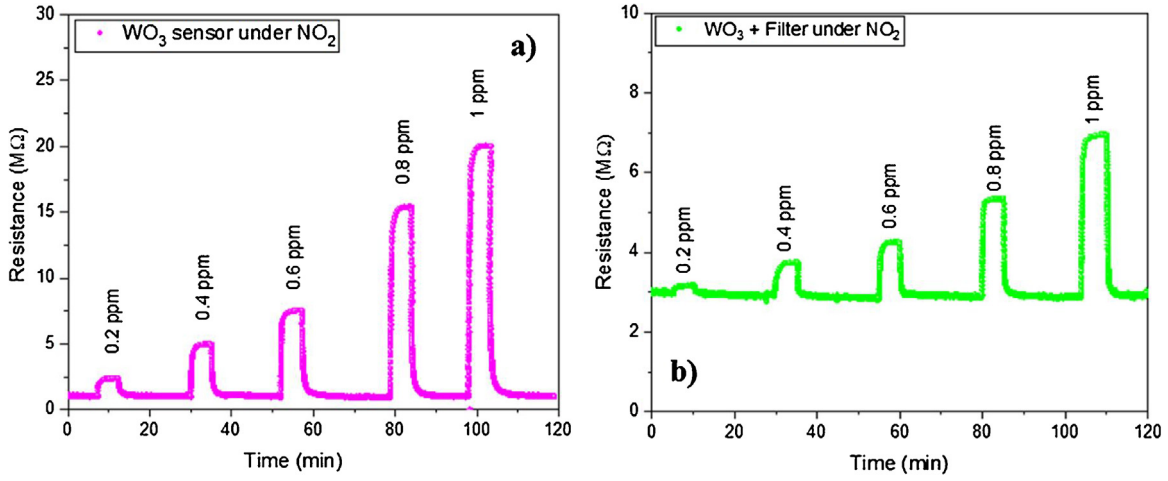

Fig. 5. Response of WO_3 gas sensor at 275 °C coupled with F2 (1.79 g) under NO_2: a) without filter and b) with filter.

Table 2
O_3 and NO_2 efficiency trapping for various filters with 1.79 g of nanoporous material.

		[O_3] = 210 ppb Trapping efficiency (%)	[NO_2] = 1.0 ppm Trapping efficiency (%)	Sensor stabilization Time (min)
Sensor + Filter	F1	100	60.5	125.2
	F2	100	58	73
	F3	100	100	149
	F5	100	61.6	349.5
	F6	100	62	269.5
	F7	96.9	26.2	79.3
	F8	98	48	67.5
Sensor without Filter		–	–	45.2

stabilization time of the sensor. This time is defined as the time required for the sensor to reach an equilibrium state under air.

The results clearly indicate a much higher filtering efficiency under O_3 than NO_2. Except for F7 and F8, all filters can trap easily O_3 molecules. Note that F3 can trap efficiently both O_3 and NO_2 molecules.

To have a closer look at the filters efficiency, four filters (F1, F2, F5 and F7) have been selected for further tests under ozone with less filtering material 0.2 g instead of 1.79 g. The purpose of such test is to determine if the filters can still completely trap ozone molecules. In Fig. 4, the responses to ozone of the sensor coupled with the different filters are illustrated. The open rectangles in Fig. 4-a--c indicates the moment the ozone was injected.

When decreasing the filtering material to 0.2 g, F1 and F5 still display a 100% efficiency for ozone trapping as illustrated in Fig. 4-a and -b, while F7 shows a poor efficiency. F2 remains 100% efficient up to 80 ppb of ozone but its trapping efficiency decreases to ~75 ± 5% above this concentration (Fig. 4-c). Among F1, F2 and F5, F2 is the filter that traps the less NO_2 (see Table 2). Moreover, the stabilization time of the WO_3 sensor is the fastest with F2 filter as compared to F1 and F5. For these reasons, F2 appears as the most promising filter for the study of the selectivity of the MOX sensors under NO_2. The following studies aim at further testing the possibility of detecting NO_2 with F2 in dry and wet air (50% RH, T=32 °C).

When F2 filter (1.79 g) is coupled upstream with the sensor and is exposed to dry gas mixture, the amount of NO_2 detected is smaller than in the absence of filter indicating that NO_2 is partly trapped in the filter (Fig. 5). One can note that the amount of trapped NO_2 increases with the initial NO_2 concentration in the gas mixtures.

When the gas mixtures are humidified at 50% relative humidity (measured in the thermo-regulated test chamber at 32° C), the sensor response remains quite similar over the same domain of NO_2 concentration (compare Fig. 5-b with Fig. 6). This result is explained in terms of the capability of F2 to partially trap humidity.

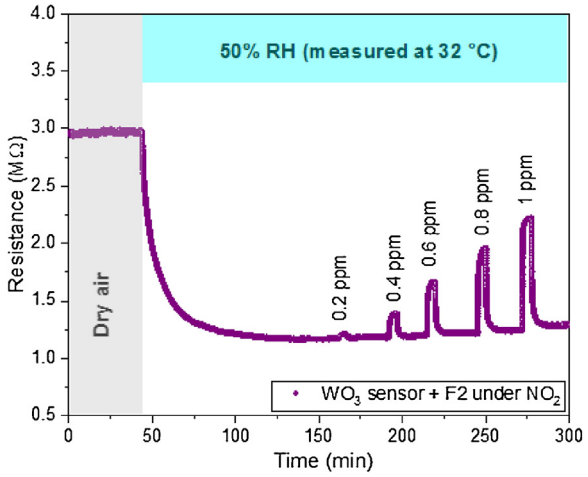

Fig. 6. Response of the sensor at 275 °C with F2 (1.79 g) for NO_2 trapping efficiency under RH = 50% rich atmosphere (RH measured at 32 °C).

In fact, despite the induced hydrophobicity of the hybrid silicate materials due to the presence of phenyl groups, the porous filter F2 can retain partially water molecules. Therefore, the real humidity that sense the WO_3 MOX was strongly reduced as compared to the initial one (RH = 50%). Furthermore, metal oxides do not react in the same way in the presence of humidity. In the case of WO_3, several study have shown that this material is only slightly affected by low humidity (<50% RH) [43,44].

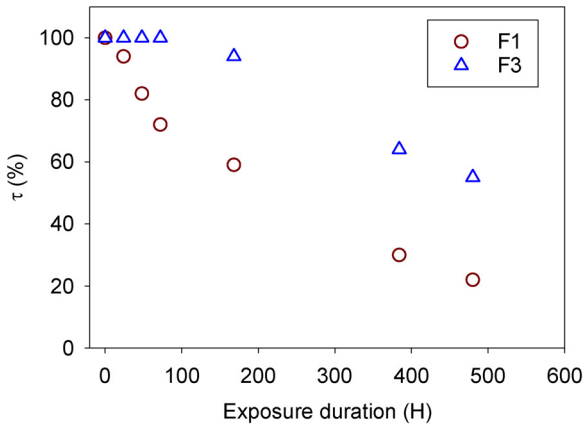

Fig. 7. Breakthrough curve for the hydrophilic F1 and hydrophobic F3 filters over 20 days. Exposure conditions: Up-stream flow: 2 L min^{-1}, $[O_3]_{up}$: 40 ± 3 ppb, HR: 50 ± 1%, T = 21 ± 1 °C.

3.4. Efficiency of O_3 trapping under various exposure conditions

The second objective of this work is to determine the potentiality of the filters for air depollution in confined environments where O_3 concentration could be high such as cars and airplanes interiors or in photocopy centers. For such studies, the lifetime and trapping efficiency of the filters under various conditions of use, i.e. high humidity and high concentrations of ozone are determined and compared to the properties of activated carbon. To measure the efficiency of ozone trapping, breakthrough curves were collected for each material under various exposure conditions. A first experiment was performed to compare the hydrophilic F1 and hydrophobic F3 matrices, both being exposed continuously during 20 days to a 2 L min^{-1} flux of air mixture containing 40 ppb of O_3 (Fig. 7). Note that the present flux is 4 times higher than the one used for the MOX sensor exposure.

The results clearly indicate a much higher filtering efficiency of the hydrophobic filter F3 than for the hydrophilic F1; after 20 days, F3 can still trap 55% of O_3 as compared to 22% for F1. Over 480H, the total amount of O_3 is 4.93 mg and the trapping efficiency of F1 and F3 is 1.47 and 2.48 mg/g of filter, respectively. Both filters are still not saturated after 20 days of exposure under humid conditions.

The photos of the filters taken at 168H show that the gradual change in color from dark blue to green to yellow is more important for the hydrophilic F1 than for the hydrophobic F3 filter. Half part of F3 filter still keep the initial blue color Fig. 8.

Since F3 is the filter that can trap efficiently both O_3 and NO_2, further tests of its resistance to humidity were undertaken; two breakthrough curves were established at high relative humidity (RH: 72%) with two different O_3 concentrations (43 and 350 ppb). The performance of F3 was compared to the efficiency of an activated carbon powder, RBAA3, which displays a high adsorption surface area of 850 ± 80 m^2 g^{-1}, 88.5% of micropores with 60% having a diameter of 11 Å and a pore volume of 0.43 ± 0.01 cm^3 g^{-1}. Both filters were continuously exposed at room temperature (T = 21 ± 1 °C) during few days to a flux of 2 L min^{-1} of air containing O_3 and a downstream measurement was performed each day.

Table 3
Comparison of F3 and AC RBAA3 trapping efficiency for O_3 at high relative humidity. Exposure conditions: Up-stream flow: 2 L min^{-1}, HR: 72 ± 2%, T = 21 ± 1 °C.

Exposure duration (H)	$[O_3]$ (ppb)	F3 (1.79 g)	AC RBAA3 (1.75 g)
24	43 ± 5	100%	100%
48	43 ± 5	100%	90%
72	43 ± 5	98%	89%
96	43 ± 5	92%	79%
Down Stream		1.27 L min^{-1}	1.16 L min^{-1}
Exposure duration (H)	**$[O_3]$ (ppb)**	**F3 (1.79 g)**	**CA RBAA3 (10.7 g)**
24	350 ± 5	100%	100%
48	350 ± 5	92%	88%
Down Stream		1.33 L min^{-1}	1.29 L min^{-1}

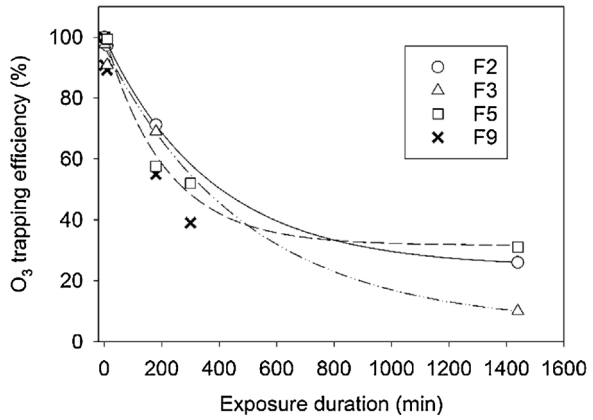

Fig. 9. Breakthrough curves of F2, F3, F5 and F9 filters exposed to O_3. Exposure conditions: Up-stream flow: 2 L min^{-1}, $[O_3]$ up: 475 ± 5 ppb, HR: 50%, T = 21 °C all samples mass: 1.79 ± 0.01 g.

It is shown that at low and high O_3 concentrations, 43 ± 5 and 350 ± 5 ppb respectively, the O_3 trapping efficiency of F3 remains higher than AC filter (see Table 3). The nanoporous filter doped with indigo carmine appears to be more resistant to high humidity than AC. This result is due to the chemical reaction between indigo carmine and O_3 that can take place in the pores whatever the humidity is. In contrast, O_3 is only adsorbed on the surface of AC and adsorption of water molecules competes at the expense of O_3 at high humidity.

Finally a comparison of the efficiency of the various hydrophobic filters was achieved with the continuous exposure of F2, F3, F5 and F9 to high concentration of O_3 (475 ppb) at RH = 50% during one day (Fig. 9). Though the difference is not drastic, it can be observed that filters which contain phenyl groups (F2, F3 and F5) appear to be efficient in contrast to F9, which displays a very low adsorption surface area.

Over 24H of exposure at a flux of 2 L min^{-1}, the total amount of O_3, which passes through each filter, is 2.93 mg and the trapping efficiency of F2, F3 and F5 are 0.87, 0.73 and 1.45 mg/g of filter, respectively. These data are consistent with the ones obtained in

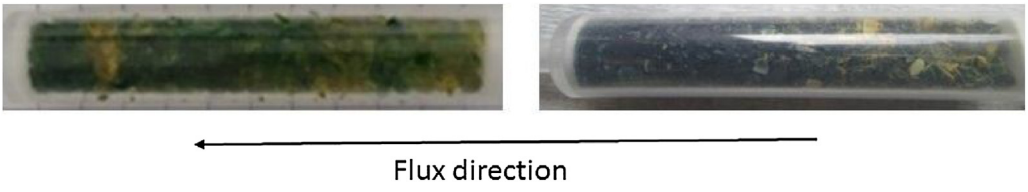

Fig. 8. Filter F1 (left) and filter F3 (right) exposed to O_3 (2 L min^{-1}, 40 ppb, RH: 50%, T = 21 °C) over 168H.

section 3.2 (compare with Fig. 4); F5 was found to be more efficient in trapping O_3 than F2. None of the filters is yet saturated.

F2, F3 and F5 whose matrices contain phenyl groups appear to display the best performances. As compared to F1 and AC RBBA (which display the highest adsorption capacity with the highest value of specific adsorption surface area ~880 $m^2 g^{-1}$ and a high percentage of micropores), the main parameter is the hydrophobicity of the matrix and the efficiency of the reaction between indigo carmine and ozone and not the porosity. F5 filter that displays a better O_3 trapping efficiency than F2 despite its smaller adsorptive capacity contains more phenyl groups than F2 and thus is more hydrophobic. All the filters, exposed to harsh conditions of O_3 concentration and humidity, had shown a good resistance to humidity and a good trapping efficiency. Their lifetimes are higher than literature values for similar filters. With indigo thin film deposited on an organic semiconductor sensor by sublimation [45], it was shown that a filter thickness of 50 nm is sufficient to trap O_3 with 99% of efficiency as compared to only 5–8% for NO_2 trapping. However, the lifetime of such thin layer is short and increasing the thickness of the layer slows down the diffusion of NO_2 through it [46]. Moreover, these authors did not determine the filter lifetime under humid conditions that could favor the co-trapping of NO_2.

4. Conclusion

The present study clearly demonstrates that nanoporous matrices doped with indigo carmine can be used as efficient filters for the trapping of ozone. The specific adsorption surface area of the nanoporous matrices is an important but not essential parameter in the trapping efficiency of O_3. The main parameters are the hydrophobicity character of the matrix that confers to the filter the resistance to humidity and the specific reaction of indigo carmine with O_3. Under very harsh conditions of exposure with high O_3 concentration and high relative humidity, the filters remain efficient in trapping O_3. By functionalizing the matrices with phenyl groups, it is possible to totally trap O_3 and partially trap NO_2. It was shown that such filters can be used upstream of MOX sensors to trap O_3 to obtain a selective NO_2 detection even in humid conditions. More works are in progress to confirm this ability with measurements of NO_2 in mixtures of O_3 and NO_2 with different proportions of the two compounds in humid gas mixtures.

Acknowledgements

The authors acknowledge the financial support of bpi-France for the project SMARTY (Smart Air Quality, contract N°165022), Dr Bernard Bonsang for providing us with the ozone generator and analyzer and Dr. Tomas Fiorido for his technical support.

References

[1] WHO Guidelines for O_3, NO_2, 2018 http://www.who.int/mediacentre/factsheets/fs313/en/.
[2] X. Gao, S. Liu, Y. Zhang, Z. Luo, M. Ni, K. Cen, Adsorption and reduction of NO_2 over activated carbon at low temperature, Fuel Process. Technol. 92 (2011) 139–146.
[3] S. Bashkova, D. Deoki, T.J. Bandosz, Effect of silver nanoparticles deposited on micro/mesoporous activated carbons on retention of NOx at room temperature, J. Colloid Interface Sci. 354 (2011) 331–340.
[4] Y. Kong, C.Y. Cha, NOx adsorption on char in presence of oxygen and moisture, Carbon 34 (1996) 1027–1033.
[5] C.J. Tighe, M.V. Twigg, A.N. Hayhurst, J.S. Dennis, Adsorption and reaction of NO_2 on carbon black and diesel soot at near-ambient temperatures, Ind. Eng. Chem. Res. 50 (2011) 10480–10492.
[6] N. Shirahama, S.H. Moon, K.H. Choi, T. Enjoji, S. Kawano, Y. Korai, et al., Mechanistic study on adsorption and reduction of NO_2 over activated carbon fibers, Carbon 40 (2002) 2605–2611.
[7] M.D. Ellison, M.J. Crotty, D. Koh, R.L. Spray, K.E. Tate, Adsorption of NH_3 and NO_2 on single-walled carbon nanotubes, J. Phys. Chem. B 108 (2004) 7938–7943.
[8] D. Li, D. Long, J. Wang, L. Ling, W. Qiao, Design of a dual-bed catalyst system with microporous carbons and urea-supported mesoporous carbons for highly effective removal of NOx at room temperature, RSC Adv. 6 (2016) 27272–27281.
[9] B.C. Dickinson, C.J. Chang, Chemistry and biology of reactive oxygen species in signaling or stress responses, Nat. Chem. Biol. 7 (2011) 504–511.
[10] A.M. Ebrahim, T.J. Bandosz, Carbon coated silica doped with cerium/zirconium mixed oxides as NO_2 adsorbent at ambient conditions, J. Phys. Chem. C 118 (2014) 8982–8992 (and therein cited refs).
[11] Z.-M. Wang, T. Arai, M. Kumagai, Cooperative and competitive adsorption mechanism of NO_2, NO, and H2O on H-type mordenite, Ind. Eng. Chem. Res. 40 (2001) 1864–1871.
[12] J. Szanyi, J. Hun Kwak, R.A. Moline, C.H.F. Peden, The adsorption of NO_2 and the NO+O_2 reaction on Na-Y, FAU: an in situ FTIR investigation, Phys. Chem. Chem. Phys. 5 (2003) 4045–4051.
[13] I. Perdana, D. Creaser, O. Öhrman, J. Hedlund, A comparison of NO_x adsorption on Na, H and BaZSM-5 films, Appl. Catal. B: Environ. 72 (2007) 82–91.
[14] A.M. Ebrahim, T.J. Bandosz, Effect of amine modification on the properties of zirconium–carboxylic acid based materials and their applications as NO_2 adsorbents at ambient conditions, Microporous Mesoporous Mater. 188 (2014) 149–162 (and therein cited refs).
[15] B. Levasseur, C. Petit, T.J. Bandosz, Reactive adsorption of NO_2 on copper-based metal-organic framework and graphite oxide/metal-organic framework composites, ACS Appl. Mater. Interfaces 2 (2010) 3606–3613.
[16] G.W. Peterson, J.J. Mahle, J.B. DeCoste, W.O. Gordon, J.A. Rossin, Extraordinary NO_2 removal by the metal–organic framework UiO-66-NH_2, Angew. Chem. Int. Ed. 55 (2016) 6235–6238.
[17] E.T. Gall, R.L. Corsi, J.A. Siegel, Impact of physical properties on ozone removal by several porous materials, Environ. Sci. Technol. 48 (2014) 3682–3690.
[18] M. Ondarts, J. Outin, L. Reinert, E. Gonze, L. Duclaux, Removal of ozone by activated carbons modified by oxidation treatments, Eur. Phys. J. Spec. Top. 224 (2015) 1995–1999.
[19] L. Berry, A. Hamwi, Activated- and temperature-controlled carbon filter to avoid interferences of ozone and nitrogen dioxide on semiconducting gas sensors, Sens. Actuators B: Chem. 150 (2010) 700–707.
[20] B. Dhandapani, S.T. Oyama, Gas phase ozone decomposition catalysts, Appl. Catal. B: Environ. 11 (1997) 129–166.
[21] G. Korotcenkov, B.K. Cho, V. Brinzari, L.B. Gulina, V.P. Tolstoy, Catalytically active filters deposited by SILD method for inhibiting sensitivity to ozone of SnO_2-based conductometric gas sensors, Ferroelectrics 459 (2014) 46–51.
[22] C. Subrahmanyam, D.A. Bulushev, L. Kiwi-Minsker, Dynamic behaviour of activated carbon catalysts during ozone decomposition at room temperature, Appl. Catal. B: Environ. 61 (2005) 98–106.
[23] T. Mathew, K. Suzuki, Y. Ikuta, Y. Nagai, N. Takahashi, H. Shinjoh, Mesoporous ferrihydrite-based iron oxide nanoparticles as highly promising materials for ozone removal, Angew. Chem. Int. Ed. 50 (2011) 7381–7384.
[24] C. Jiang, P. Zhang, B. Zhang, J. Li, M. Wang, Facile Synthesis of activated carbon-supported porous manganese oxide via in situ reduction of permanganate for ozone decomposition, Ozone: Sci. Eng. 35 (2013) 308–315.
[25] H. Valdès, S. Alejandro, C.A. Zaror, Natural zeolite reactivity towards ozone: the role of compensating cations, J. Hazard. Mater. 227–228 (2012) 34–40 (and therein-cited refs).
[26] V. Blaskov, I. Stambolova, V. Georgiev, T. Batakliev, A. Eliyas, M. Shipochka, et al., Synthesis and catalytic activity of silver-coated perlite in the reaction of ozone decomposition, Ozone: Sci. Eng. 37 (2015) 252–256.
[27] S. Yang, J. Nie, F. Wei, X. Yang, Removal of ozone by carbon nanotubes/quartz fiber film, Environ. Sci. Technol. 50 (2016) 9592–9598.
[28] J. Brunet, M. Dubois, A. Pauly, L. Spinelle, A. Ndiaye, K. Guérin, C. Varenne, B. Lauron, An innovative gas sensor system designed from a sensitive organic semiconductor downstream a nanocarbonaceous chemical filter for the selective detection of NO_2 in an environmental context. Part I: development of a nanocarbon filter for the removal of ozone, Sens. Actuators B 173 (2012) 659–667.
[29] J.A. Pauly, M. Dubois, J. Brunet, L. Spinelle, A. Ndiaye, K. Guérin, C. Varenne, A.S. Vinogradov, A. Yu Klyushin, An innovative gas sensor system designed from a sensitive organic semiconductor downstream a nanocarbonaceous chemical filter for selective detection of NO_2 in an environmental context. Part II: interpretations of O_3/nanocarbons and NO_2/nanocarbons interactions, Sens. Actuators B 173 (2012) 652–658.
[30] J. Brunet, L. Spinelle, A. Pauly, M. Dubois, K. Guerin, M. Bouvet, C. Varenne, B. Lauron, A. Hamwi, All-organic device with integrated chemical filter dedicated to the selective measurement of NO_2 in air, Org. Electron. 11 (2010) 1223–1229.
[31] J. Brunet, L. Spinelle, A. Ndiay, M. Dubois, G. Monier, C. Varenne, A. Pauly, B. Lauron, K. Guerin, A. Hamwi, Physical and chemical charactérizations of nanometric indigo layers as efficient ozone filter for gas sensor devices, Thin Solid Films 520 (2011) 971–977.
[32] K.S.W. Sing, Physisorption data for gas/solid systems with special reference to the determination of surface area and porosity, Pure Appl. Chem. 54 (1982) 2201–2218.
[33] K. Aguir, M. Bendahan, V. Laithier, Heated sensitive layer gas sensor, patent N° FR 13 59494, 2013, international extension in 2016, US20160238548A1.
[34] M. Alexy, G. Voss, J. Heinze, Optochemical sensor for determining ozone based on novel soluble indigo dyes immobilized in a highly permeable polymeric film, Anal. Bioanal. Chem. 382 (2005) 1628–1641.

[35] M.Y. Yasuko, Measurement of ambient ozone using newly developed porous glass sensor, Sens. Actuators B 126 (2007) 485–491.
[36] M.-L. calvo-Muñoz, C. Roux, F. Brunet, J.-P. Bourgoin, A. Ayral, A. El-Mansouri, T.-H. Tran-Thi, Chemical sensors of monocyclic aromatic hydrocarbons based on sol-gel materials: synthesis, structural characterization and molecular interactions, J. Mater. Chem. 12 (2002) 461–467.
[37] P.I. Ravikovitch, A.V. Neimark, Density functional thery model of adsorption on amorphous and microporous silica material, Langmuir 22 (2006) 11171–11179.
[38] D.J. Smith, J.F. Vetelino, R.S. Falconer, E.L. Wittman, Stability, sensitivity and selectivity of tungsten trioxide films for sensing applications, Sens. Actuators B 13–14 (1993) 264–268.
[39] M. Penza, M.A. Tagliente, L. Mirenghi, C. Gerardi, C. Martucci, G. Cassano, Tungsten trioxide (WO_3) sputtered thin films for a NOx gas sensor, Sens. Actuators B 50 (1998) 9–18.
[40] T. Nguyen, S. Park, J.B. Kim, T.K. Kim, G.H. Seong, J. Choo, Y.S. Kim, Polycrystalline tungsten oxide nanofibers for gas-sensing applications, Sens. Actuators B 160 (2011) 549–555.
[41] J. Guérin, M. Bendahan, K. Aguir, A dynamic response model for the WO_3-based ozone sensors, Sens. Actuators B 128 (2008) 462–467.
[42] A. Labidi, C. Lambert-Mauriat, C. Jacolin, M. Bendahan, M. Maaref, K. Aguir, dc and ac characterizations of WO_3 sensors under ethanol vapors, Sens. Actuators B 119 (2006) 374–379.
[43] C.S. Rout, K. Ganesh, A. Govindaraj, C.N.R. Rao, Sensors for the nitrogen oxides, NO_2, NO and N_2O, based on In_2O_3 and WO_3 nanowires, Appl. Phys. A 5 (2006) 241–246.
[44] Z. Ling, C. Leach, The effect of relative humidity on the NO_2 sensitivity of a SnO_2/WO_3 heterojunction gas sensor, Sens. Actuators B 102 (2004) 102–106.
[45] J. Brunet, L. Spinelle, A. Pauly, M. Dubois, K. Guerin, M. Bouvet, C. Varenne, B. Lauron, A. Hamwi, All-organic device with integrated chemical filter dedicated to the selective measurement of NO_2 in air, Org. Electron. 11 (2010) 1223–1229.
[46] J. Brunet, L. Spinelle, A. Ndiay, M. Dubois, G. Monier, C. Varenne, A. Pauly, B. Lauron, K. Guerin, A. Hamwi, Physical and chemical characterizations of nanometric indigo layers as efficient ozone filter for gas sensor devices, Thin Solid Films 520 (2011) 971–977.

Biographies

M. Othman received the MSc degree in 2011 from the University of Tunis El Manar (Tunis, Tunisia). He was awarded his PhD in 2015° in Micro and Nanoelectronics from Aix-Marseille University (France), where he was working as a Postdoctoral researcher in the μSensors team of the Institut Materiaux, Microelectronique & Nanosciences de Provence (IM2NP–CNRS). He is currently working as a Postdoctoral Fellow at Aix-Marseille University at LSIS Lab. His main areas of research interest are selectivity of MOX gas sensors, semiconductors physics and reliability of electronics components.

C. Théron received his Ph.D. degree in 2013 at École Nationale Supérieure de Chimie of Montpellier, France. He then conducted postdoctoral studies with Pr. C. J. Brinker at the University of New Mexico, USA. From 2015 to 2017, he joined the Chemical Sensors team (UMR 3685 NIMBE) at CEA-Saclay as a post-doctoral researcher. He is currently leading research in the Lotus Synthesis start-up. His research interests include design and applications of hybrid materials, mesoporous materials and organosilica nanocomposites.

M. Bendahan is a Professor at Aix-Marseille University (France). He is currently the head of the Microsensors Team at the Institute of Materials Microelectronic Nanosciences of Provence (IM2NP-CNRS) at Aix-Marseille University, Marseille (France). He is also a Lecturer in electronics at the Institute of Technology of Marseille (head of the electronic department from 2009 to 2015). He was awarded his PhD degree from the University of Aix-Marseille in 1996 with a thesis on shape memory alloys thin films for micro-actuator applications. He is specialized in thin films preparation and characterization for applications in microsystems. His principal research interest is now directed towards the conception, realization and the electrical characterization of microsensors: gas microsensors based on inorganic metal–oxides (WO3, ZnO, CuO, SnO2. . .) and organic materials, flexible temperature sensors and flexible pressure sensors.

C. Rivron is a CNRS Assistant-engineer in UMR 3685 NIMBE at CEA-SACLAY. He is a specialist of porosimetry and is in charge of the characterization of new materials developed in the Chemical Sensors team.

S. Bernardini is a Lecturer at Aix-Marseille University (France). She received (i) her M.S. degrees in fundamental physics from Paul Cezanne University, Marseille, France in 1999, (ii) her Engineering degree in materials and microelectronics from the National Institute of Applied Sciences (INSA), Lyon, France, in 2001, and (iii) her Ph.D. degree in microelectronics from Provence University, Marseille, in 2004. From 2005 to 2007, she moved to the Microelectronic and Nanostructure group at the University of Manchester (UK), where she was involved in structural and electrical characterizations to study reliability, interface degradation and impact of high-k dielectrics on carrier transport in MOSFETs. From 2007 to 2008, she characterized nanometric systems based on zinc oxide nanorods at the Nanoscience Center of Marseille (CINaM). In 2008, she joined the Sensors Group as Lecturer at the Institute Materials and Microelectronic Nanoscience of Provence (IM2NP). Her current interests and activities cover the engineering and physics of gas sensors and selectivity enhancement strategies.

G. Le Chevallier is currently a CNRS engineer inUMR 3685 NIMBE at CEA-Saclay. He is in charge of the development of set-up for experimental test benches and IT software for data processing in the Chemical Sensors team.

E. Chevallier received his PhD degree in Chemistry/Physics in 2003 at the University of Jussieu (France). From 2004 to 2010 he worked with Atomic energy Commission (CEA) in the development of chemical sensors and analysis methods for the detection of toxic chemical agents. From 2010 to 2016 he joined ETHERA as scientific manager in charge of R&D solutions for indoor air chemical pollution diagnosis and treatment. He is currently Head of Environment, Pollution, Chemical and Sustainable-Development at French National Institute for Consumer Affairs (INC).

K. Aguir is a Professor at Aix Marseille University (France). He was awarded his Doctorat d'Etat ès Sciences degree from Paul Sabatier University, Toulouse (France) in 1987. He was during the 16 years the head of Microsensors Group at the Institute of Materials Microelectronic Nanosciences of Provence (IM2NP-CNRS) at Aix-Marseille University, Marseille (France). His principal research interests are directed towards metal – oxide (WO3, SnO2, SrTiO3, CuO, ZnO) and organic thin films for gas sensors, flexible gas sensors, microsystems, selectivity enhancement strategies including surface modification of sensors, signal treatment, adsorption – desorption noise spectroscopy, modeling of gas sensor responses analysis, flexible current sensors, ultra-low power and wireless systems. He is the author of over 200 publications and international conferences. Referee of several scientific journals, he has conducted numerous expertise and he is a member of scientific committees of international conferences.

T-H. Tran-Thi received her Doctorat ès-Sciences Physiques degree in Radiation Chemistry in 1983 at the University of Paris XI. She is presently Director of Research and leads the Chemical Sensors team in UMR 3685 NIMBE, a unit of the Atomic energy Commission (CEA-Saclay) associated with the National Council of Scientific Research (CNRS). She is also the scientific counsellor of ETHERA, a CEA-CNRS spin-off that she co-founded in 2010 with two CEA colleagues.